Chapter 4

Initial Stresses in Rocks and Their Measurement

Any undisturbed mass of rock in situ contains nonzero stress components due to weight of overlying materials, confinement, and past stress history. Near the surface in mountainous regions the in situ stress may approach zero at some points or lie close to the rock strength at others. In the former case, rocks may fall from surface and underground excavations because joints are open and weak; in the latter case, disturbance of the stress field by tunneling or perhaps even surface excavation may trigger violent release of stored energy. This chapter concerns determination of the magnitude and direction of the initial stresses at the site of a work.

4.1 Influence of the Initial Stresses

It is often possible to estimate the order of magnitude of stresses and their directions, but one can never be certain of the margin of error without backup measurements. Application of such measurements is fairly common in mining practice, but since stress measurements tend to be expensive they are not routine for civil engineering applications. There are several civil engineering situations, however, when knowledge of the state of stress can be helpful or lack of knowledge might prove so costly that a significant stress measurement program is warranted. For example, when choosing the *orientation* for a cavern, one hopes to avoid aligning the long dimension perpendicular to the greatest principal stress. If the initial stresses are very high, the *shape* will have to be selected largely to minimize stress concentrations. Knowledge of rock stresses also aids in *layout* of complex underground works. An underground power-

house for example, consists of a three-dimensional array of openings including a machine hall, a transformer gallery, low-voltage lead shafts, pressure tunnels, surge shafts, rock traps, access tunnels, ventilation tunnels, muck hauling tunnels, penstocks, draft tubes, and other openings. Cracks that initiate at one opening must not run into another (Figure 4.1*a*). Since cracks tend to extend in the plane perpendicular to σ_3 knowledge of the direction of the stresses permits choosing a *layout* to reduce this risk. Pressure tunnels and penstocks can be constructed and operated in rock without any *lining* if virgin stress is greater than the internal water pressure, so for such applications stress measurement might permit large cost savings. When *displacement instruments* are installed in an underground or surface excavation, to monitor the rock performance during construction and service, stress measurements beforehand provide a framework for analysis of the data and enhance their value. When making large surface excavations with *presplitting* techniques, economies will be realized if the excavation is oriented perpendicular to σ_3 (Figures 4.1*b*,*c*). With underground storage of fluids in reservoir rocks, knowledge of the initial state of stress will help evaluate the potential hazard of *triggering an earthquake*. These are a few examples of situations in which a knowledge of the state of stress can be integrated in engineering design. In a more general sense, however, the state of stress can be considered a basic rock attribute whose magnitudes and directions affect the overall rock strength, permeability, deformability, and other important rock mass characteristics. Thus it is rarely irrelevant to know the initial stress state when dealing with rock in situ.

Sometimes initial stresses are so high that engineering activities can trigger rock failure. Whenever the major stress in the region of an excavation is more than about 25% of the unconfined compressive strength, new cracking can be expected as a result of construction no matter how carefully it is performed. This derives from two observations: (1) the maximum stress concentration around an underground opening cannot be less than 2; and (2) cracking occurs in an unconfined compression specimen when the stress reaches about half of the unconfined compressive strength. Close to steep valley sides, where the angle from the excavation to the mountain top is greater than 25°, data show that rock stress problems tend to occur in Norwegian fjord country whenever the weight of rock cover is greater than about $0.15q_u$ (Brekke and Selmer-Olsen, 1966; Brekke, 1970). Such stress problems can vary from slabbing and overbreak of rock on the tunnel wall nearest the valley side, to isolated violent detachment of rocks from the walls or even destructive bursts. Conditions for rock bursts are found underground in deep mines, as in the Canadian Kirkland Lake District, the South African gold mines, and the Idaho Coeur d'Alene district, where mining is pursued at depths of as much as 11,000 ft. In civil engineering work, in addition to the valleyside stress problem noted, railroad and road tunnels under high mountains, such as, the Mont Blanc Tunnel in the Alps, have encountered severe rock stress problems. In shales and other rocks

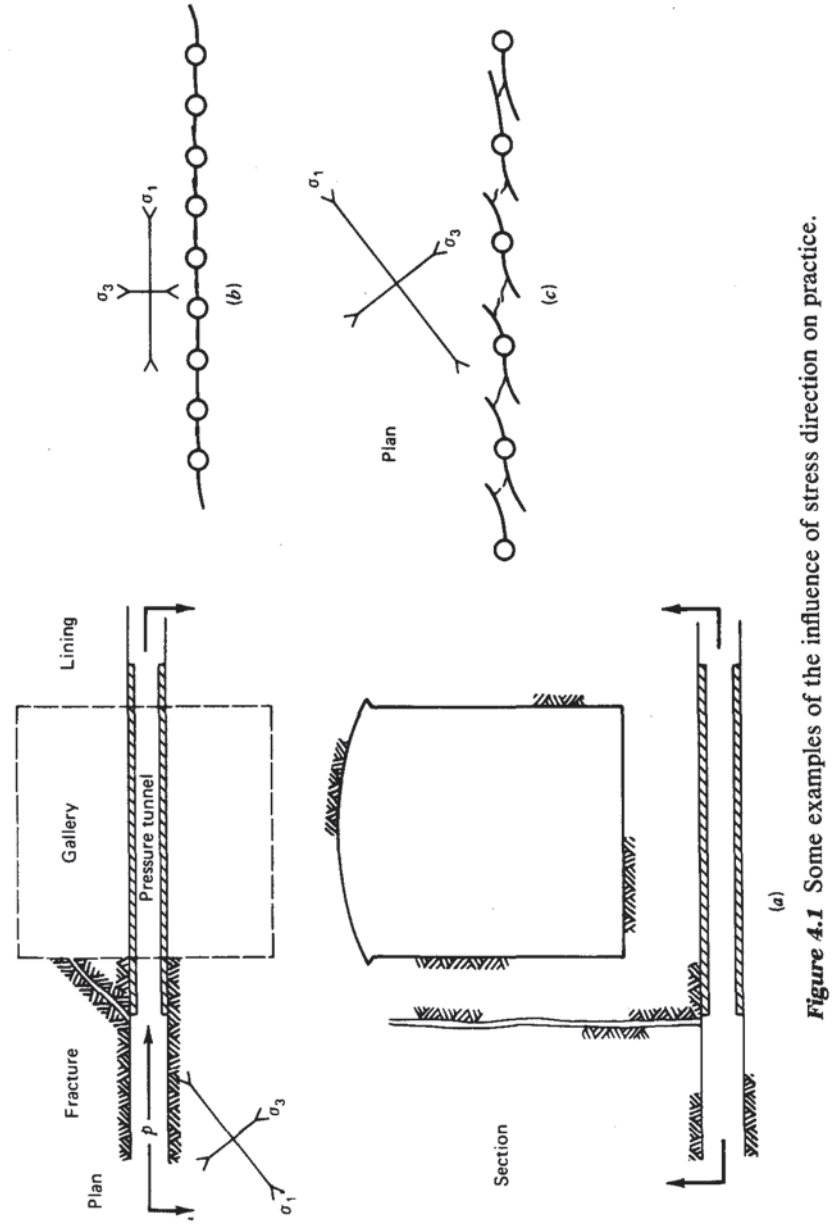

Figure 4.1 Some examples of the influence of stress direction on practice.

with low values of q_u, conditions for rock failure due to concentration of initial stress may lead to slow compression ("squeeze") and destruction of tunnel supports rather than violent collapse, but difficulties can still be significant. The "stand-up time" of a tunnel, that is, the maximum duration for erecting supports, is closely related to the ratio of maximum initial stress to q_u.

4.2 Estimating the Initial Stresses

VERTICAL STRESS

It is generally safe to assume that the vertical normal stress is equal to the weight of the overlying rock, 0.027 MPa/m or 1.2 psi/ft on the average. Near horizontal ground, the principal stress directions are vertical and horizontal. It is often assumed that they are also vertical and horizontal at depth (Figure 4.2*a*); however, this is just an assumption to reduce the number of unknowns, an assumption that finds reinforcement in Anderson's observations that normal and reverse faults often dip at 60 and 30°, respectively (see Jaeger and Cook, 1976). The simplifying assumption that the principal stresses are vertical and horizontal has been widely adopted in practice. Of course, this breaks down at shallow depths beneath hilly terrain, because the ground surface, lacking normal and shear stresses, always forms a trajectory of principal stress (Figure 4.2). Beneath a valley side, one principal stress is normal to the slope and equals zero, while the other two principal stresses lie in the plane of the slope

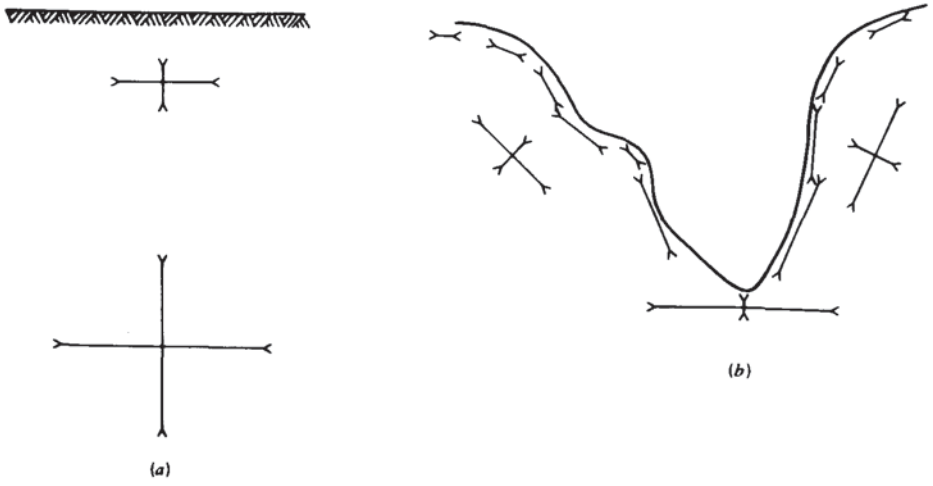

Figure 4.2 The influence of topography on initial stresses.

(Figure 4.2*b*). These stresses likewise approach zero where the rock slope is convex upward but grow larger where the slope is concave upward. Beneath the sharp notch of a V-shaped valley, the in situ stresses may be close to or at the strength of the rock.

Over any significant horizontal surface within the ground, the average vertical stress must equilibrate the downward force of the weight of overlying rock, hence the rule stated previously:

$$\bar{\sigma}_v = \gamma Z \tag{4.1}$$

where $\bar{\sigma}_v$ is the average total vertical stress at depth Z in rock with unit weight γ. This rule has been supported by numerous measurements (Figure 4.7*a*) and is one of the reliable formulas of stress in situ. However, it can be violated over limited horizontal distances owing to effects of geological structure. Figure 4.3, for example, shows how the vertical stress might vary along horizontal planes cutting through a succession of rigid and compliant beds folded into synclines and anticlines. Along line AA' the stress varies from perhaps 60% greater than γZ under the syncline to zero just beneath the anticline, the more rigid layer serving as a protective canopy and directing the flow of force down the limbs of the fold. A tunnel driven along line BB' could expect to pass from relatively understressed rock in the compliant shales to highly stressed rock as it crossed

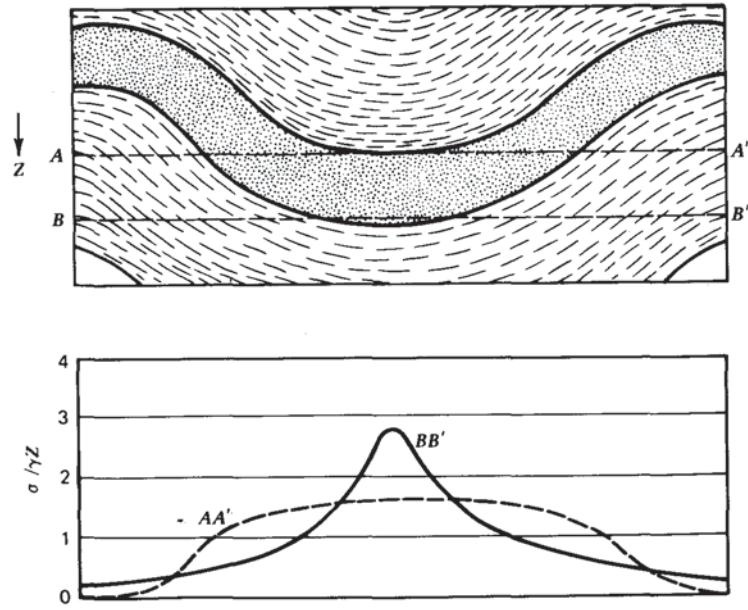

Figure 4.3 The influence of folds in heterogeneous, layered rock on vertical stresses.

into more rigid sandstone in passing under the trough of the syncline. If there is a low-strength sheared zone along the contact, produced by slip between the layers during folding, the vertical stress could be expected to jump in crossing the contact. Since geological structure can alter the vertical stresses and the direction of principal stresses, it is wise to investigate geological effects through analysis in important applications wherever geological heterogeneities can be expected to deflect the lines of force away from the vertical. Figure 4.4 shows the result of one such analysis, performed using the finite element method, in a region with heterogeneous geology superimposed on a sharply notched topography.

HORIZONTAL STRESS

In regard to the magnitude of the horizontal stresses, it is convenient to discuss the ratio of horizontal to vertical stresses. Let

$$K = \frac{\sigma_h}{\sigma_v} \tag{4.2}$$

In a region of recent sedimentation, such as the Mississippi Delta, the theory of elasticity can be invoked to predict that K will be equal to $\nu/(1 - \nu)$. This expression derives from the symmetry of one-dimensional loading of an elastic material over a continuous plane surface, which infers a condition of no horizontal strain; such a formula has no validity in a rock mass that has experienced cycles of loading and unloading. Consider an element of rock at depth Z_0 with initial value of $K = K_0$, which is then subjected to unloading by removal of ΔZ thickness of overburden (Figure 4.5). Due to unloading of $\gamma \Delta Z$ vertical stress, the horizontal stress is reduced by $\gamma \Delta Z \nu/(1 - \nu)$. Therefore, after erosion of a thickness of rock equal to ΔZ, the horizontal stress at depth $Z = Z_0 - \Delta Z$ will become equal to $K_0 \gamma Z_0 - \gamma \Delta Z \nu/(1 - \nu)$, and

$$K(Z) = K_0 + \left[\left(K_0 - \frac{\nu}{1 - \nu}\right) \Delta Z\right] \cdot \frac{1}{Z} \tag{4.3}$$

Thus, erosion of overlying rock will tend to increase the value of K, the horizontal stress becoming greater than the vertical stress at depths less than a certain value.[1] The hyperbolic relationship for $K(Z)$ predicted by Equation 4.3 can be generated by other arguments. While the vertical stress is known to equal γZ, the horizontal stress could lie anywhere in the range of values between the two extremes $K_a \sigma_v$ and $K_p \sigma_v$ shown in Figure 4.6. K_a corresponds to conditions for normal faulting, Figure 4.6*b*, in which the vertical stress is the

[1] With the restriction $K \leq K_p$ given by (4.5). Thermal effects have been ignored.

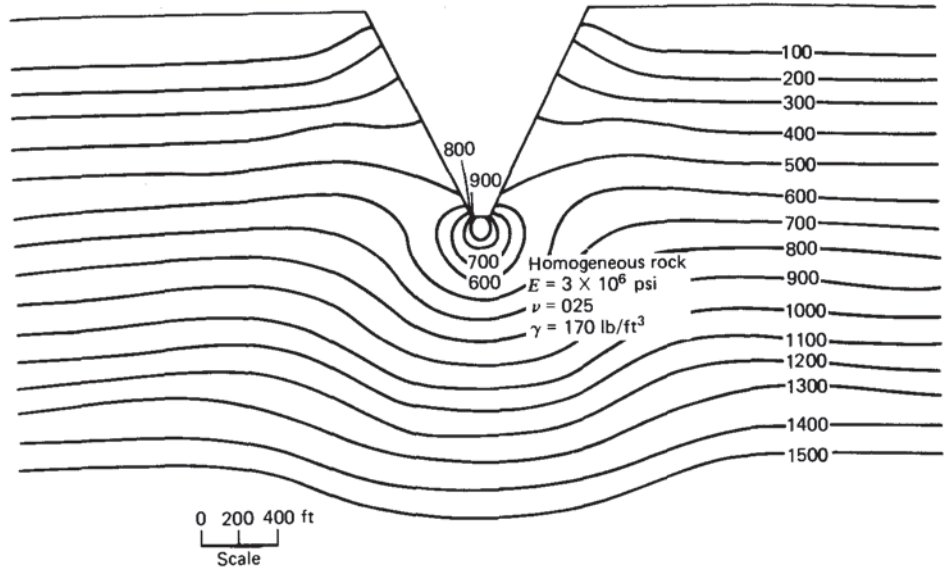

(*a*)

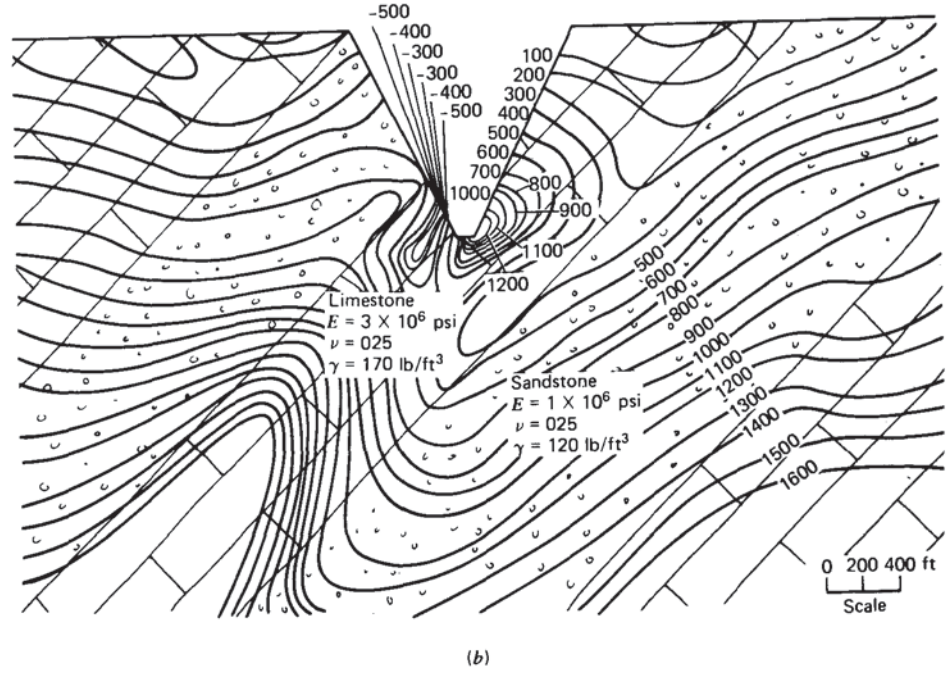

(*b*)

Figure 4.4 Comparison of maximum shear stresses beneath valleys in homogeneous (*a*) and heterogeneous (*b*) formations. Units of shear stress are hundreds of pounds per square foot.

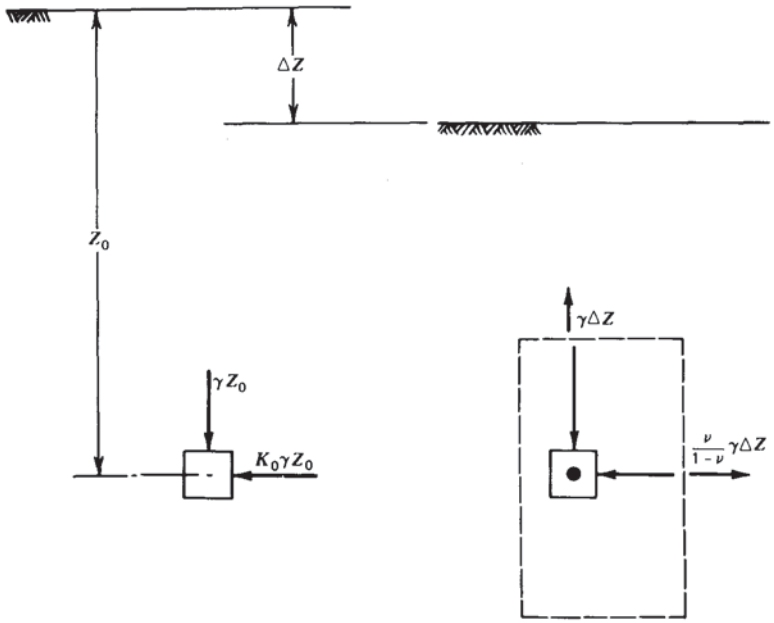

Figure 4.5 The effect of erosion on stresses at depth.

major principal stress and failure is by horizontal extension. Assuming Coulomb's law

$$K_a = \text{ctn}^2\left(45 + \frac{\phi}{2}\right) - \left[\left(\frac{q_u}{\gamma}\right)\text{ctn}^2\left(45 + \frac{\phi}{2}\right)\right] \cdot \frac{1}{Z} \tag{4.4}$$

K_p corresponds to conditions for reverse faulting (Figure 4.6*c*), in which the vertical stress is the minor principal stress and failure is by horizontal compression, giving

$$K_p = \tan^2\left(45 + \frac{\phi}{2}\right) + \frac{q_u}{\gamma} \cdot \frac{1}{Z} \tag{4.5}$$

Values of these extreme horizontal stresses are tabulated for an assumed set of rock properties in Table 4.1. If there is no existing fault, we observe that the range of possible values of K such that $K_a \leq K \leq K_p$ is quite vast. However, near a preexisting fault, q_u can be assumed equal to zero and the range of K is considerably reduced. Although tension is possible, it has rarely been measured and is to be considered an unusual situation.

Brown and Hoek (1978) examined a number of published values of in situ

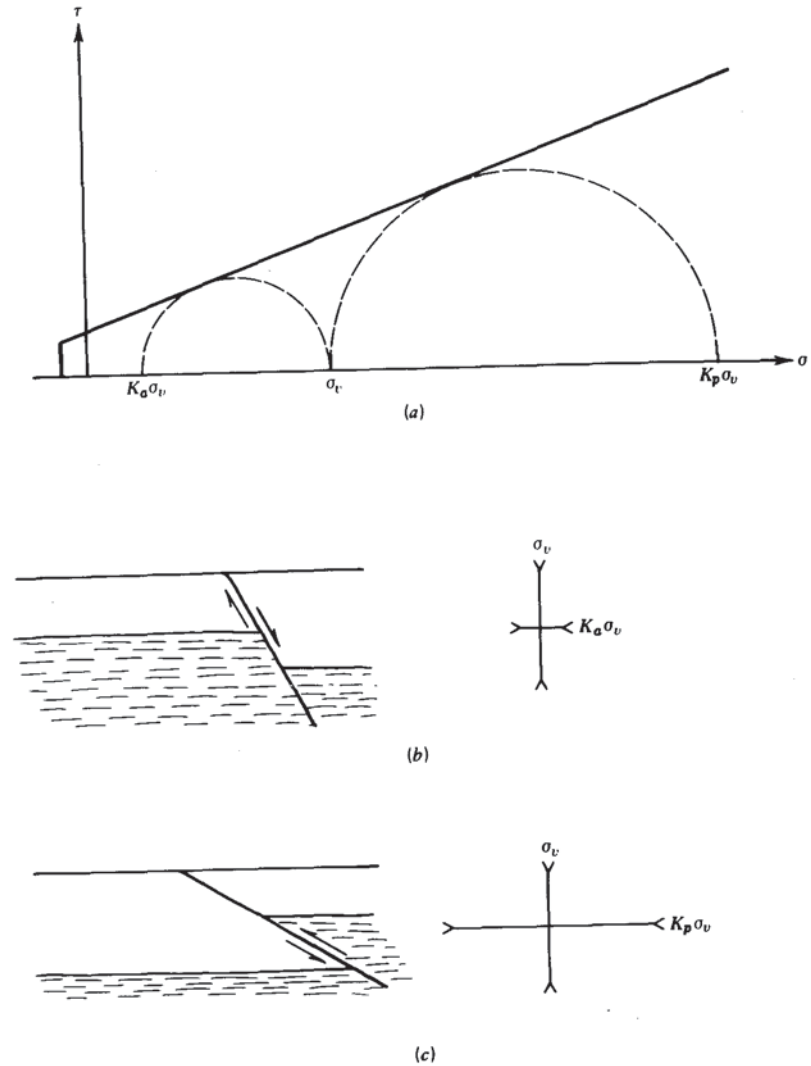

Figure 4.6 Stresses required to initiate normal and reverse faults.

stress (Figure 4.7*b*) and independently discerned a hyperbolic relation for the limits of $K(Z)$, as

$$0.3 + \frac{100}{Z} < \overline{K} < 0.5 + \frac{1500}{Z} \tag{4.6}$$

where Z is the depth in meters and $\overline{K}$ is the ratio of average horizontal stress to vertical stress. The range in extreme values of $\overline{K}$ given by this empirical crite-

***Table 4.1** Extreme Values for Possible Horizontal Stresses Corresponding to Conditions for Normal and Reverse Faulting $\gamma = 25.9\ kN/m^3$*

		Before Faulting Occurs; No Preexisting Fault Horizontal Stress σ_h				After Faulting Has Occurred and a Fault Exists Horizontal Stress σ_h			
		q_u = 13.8 MPa, ϕ = 40°		q_u = 2 MPa, ϕ = 20°		q_u = 0, ϕ = 40°		q_u = 0, ϕ = 20°	
Depth (m)	Vertical Stress σ_v (MPa)	Normal Faulting (MPa)	Reverse Faulting (MPa)	Normal Faulting (MPa)	Reverse Faulting (MPa)	Normal Faulting (MPa)	Reverse Faulting (MPa)	Normal Faulting (MPa)	Reverse Faulting (MPa)
10	0.26	−2.94	14.99	−0.85	2.53	0.06	1.19	0.13	0.53
20	0.52	−2.88	16.18	−0.73	3.06	0.11	2.38	0.25	1.06
40	1.04	−2.77	18.56	−0.47	4.11	0.23	4.76	0.51	2.11
60	1.55	−2.66	20.95	−0.22	5.17	0.34	7.15	0.76	3.17
100	2.59	−2.43	25.72	0.29	7.28	0.56	11.91	1.27	5.28
150	3.89	−2.15	31.68	0.92	9.92	0.84	17.87	1.90	7.92
200	5.18	−1.87	37.64	1.56	12.57	1.13	23.82	2.54	10.57
400	10.36	−0.74	61.49	4.10	23.13	2.25	47.64	5.08	21.13
750	19.43	1.23	103.2	8.54	41.62	4.22	89.33	9.52	39.62
1000	25.90	2.64	133.0	11.72	54.83	5.63	119.1	12.70	52.83
2000	51.80	8.28	252.4	24.42	107.6	11.26	238.2	25.40	105.6

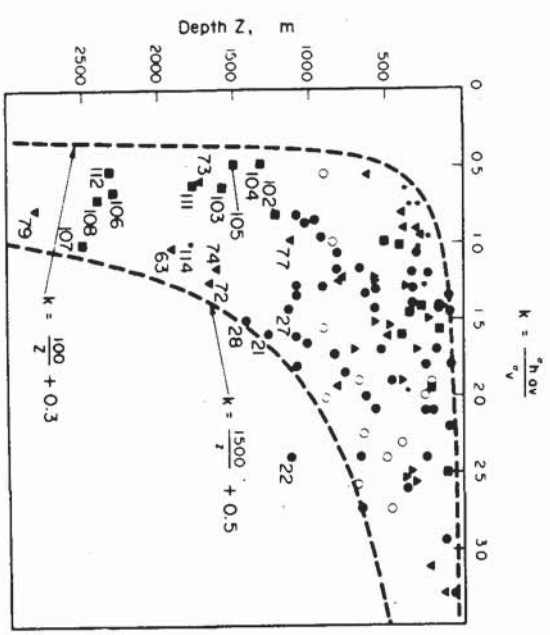

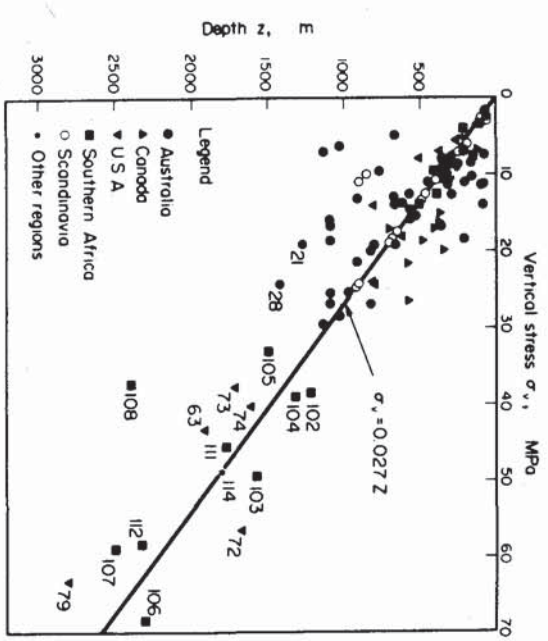

***Figure 4.7** Results of stress measurements. (a) Vertical stresses. (b) Average horizontal stresses [(a) and (b) from Brown and Hoek, (1978).]*

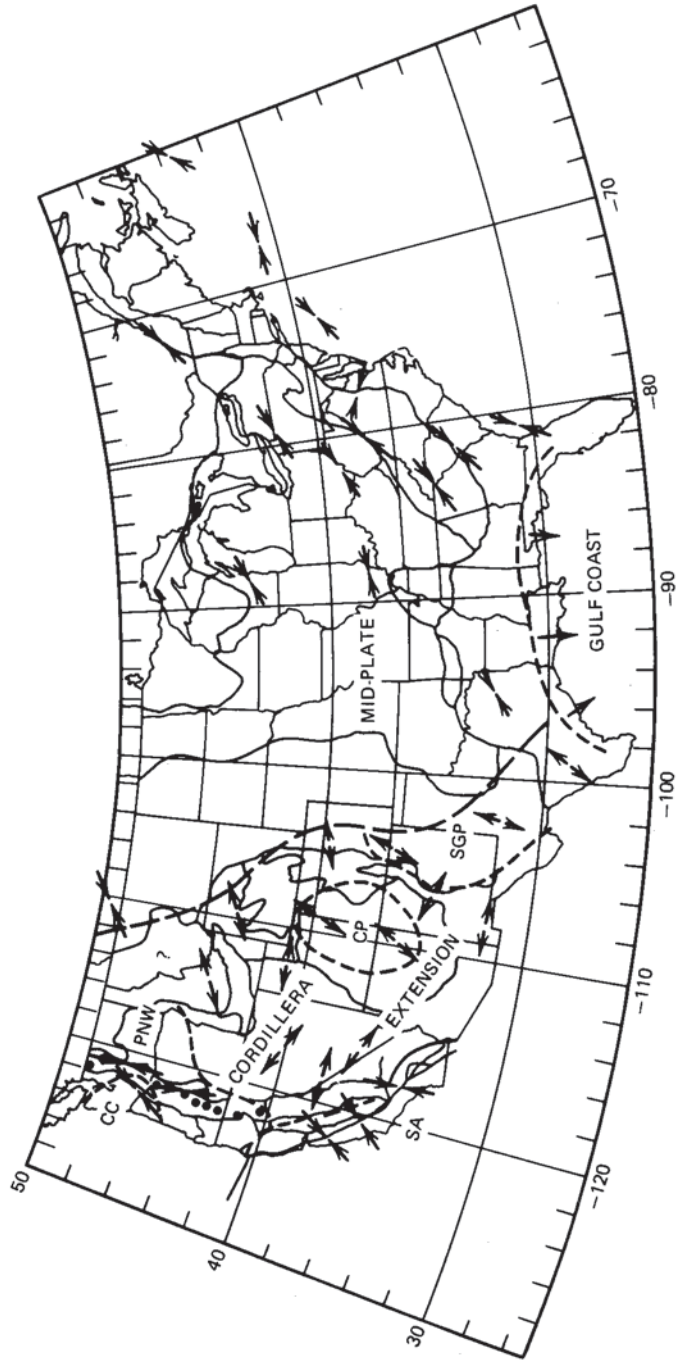

Figure 4.7 Results of stress measurements. (*c*) Directions of greatest stress in compression regions (inward directed arrows) and of least stress in extension regions (outward directed arrows). From Zoback and Zoback (1988) with permission.

rion is considerably less than the range K_a to K_p given by (4.4) and (4.5) when q_u is not equal to zero, due in part to the fact that average horizontal stress is being considered, whereas the previous criteria refer to maximum and minimum values of horizontal stress. In any event, all the equations for $K(Z)$ presented and the actually measured data are consistently found to be inverse with Z. Thus, even without measurements one can estimate, within broad limits, the variation of horizontal stress with depth. While the *magnitude* of the horizontal stress might be estimated only approximately, it is often possible to offer good estimates for the *directions* of the horizontal stresses.

HORIZONTAL STRESS DIRECTION

If the present state of stress is a remnant of that which caused visible geological structure, it will be possible to infer the directions of stresses from geological observations. Figure 4.8 shows the relationship between principal stress directions and different types of structures. The state of stress that causes a normal fault has σ_1 vertical, and σ_3 horizontal pointed perpendicularly to the fault trace as seen in the plan. In the case of reverse faulting, the stresses that caused the rupture have σ_3 vertical, while σ_1 is horizontal and directed perpendicular to the fault trace. Axial planes of folds also define the plane of greatest principal stress. Strike-slip faults are created by a state of stress in which σ_1 is horizontal and inclined about 30° with the fault trace, clockwise or counterclockwise as dictated by the sense of motion on the fault. These directions of horizontal stresses are not those of crustal blocks caught and squeezed between pairs of parallel faults; in such blocks, the primary stress state of the crust that is linked directly to the primary rupture surfaces will have superimposed on it the effects of the strain from accumulated fault motions, as discussed by Moody and Hill (1956).

Another line of observations comes from dikes and flank volcanoes formed around larger craters. Some dikes represent hydraulic fractures, in which case they lie perpendicular to σ_3. The perpendicular to a radius from a master crater to a flank volcano similarly identifies the direction of least horizontal stress.[2] Seismologists are able to indicate the directions of primary stresses from first motion analysis of earthquakes. If the directions of the vectors from the focus to different seismic stations are plotted on a stereographic projection of a unit reference hemisphere, it will be seen that two regions contain vectors to stations that received compressive first motion, while the other two regions contain vectors that received extensile first motion (Figure 4.8*f*). Two great circles are drawn to divide these fields and their point of intersection defines the direction of σ_2. The direction of σ_1 is 90° from the direction of σ_2 approxi-

[2] K. Nakamura (1977) Volcanoes as possible indicators of tectonic stress orientation—Principle and proposal. *J. Volcanol. Geothermal Res.* **2**: 1–16.

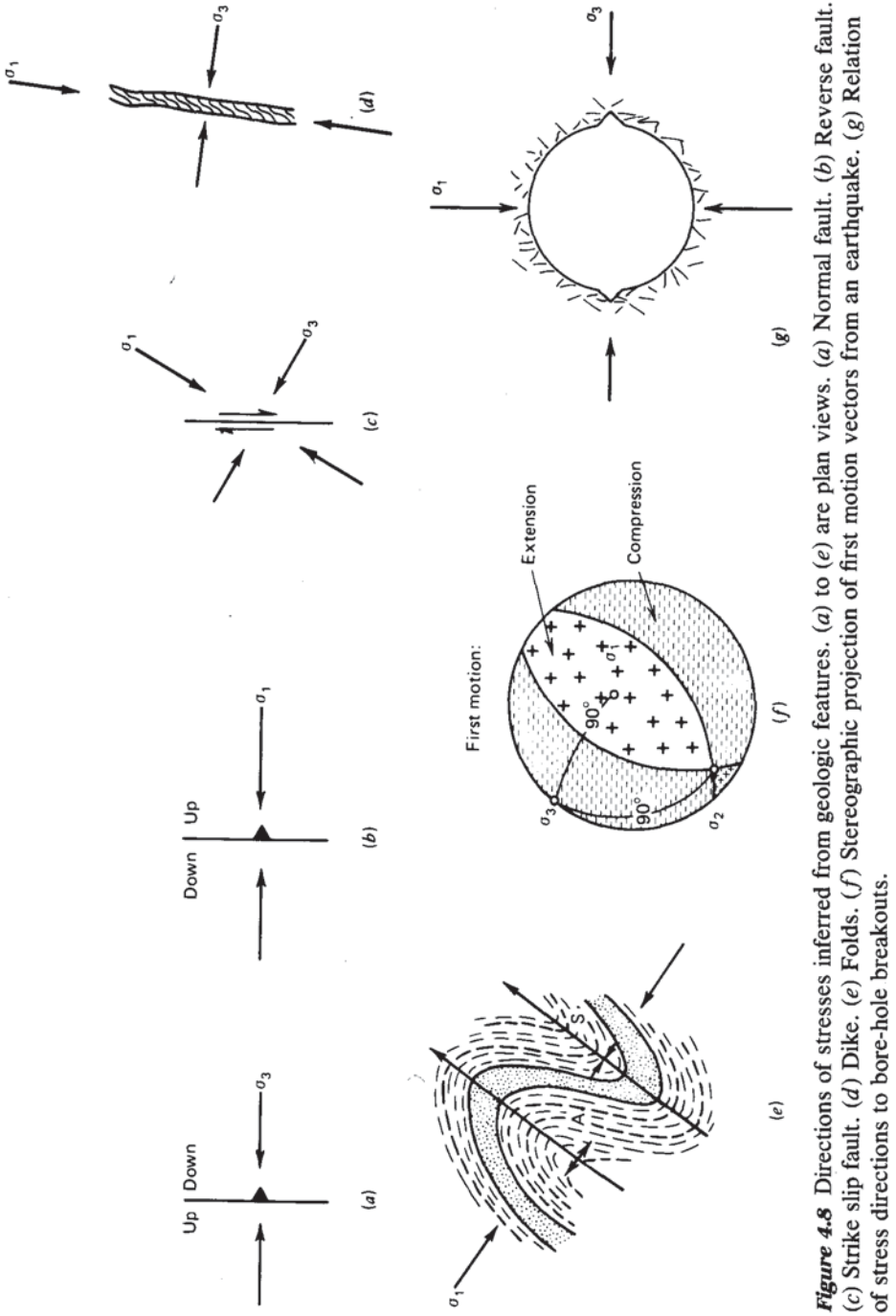

Figure 4.8 Directions of stresses inferred from geologic features. (*a*) to (*e*) are plan views. (*a*) Normal fault. (*b*) Reverse fault. (*c*) Strike slip fault. (*d*) Dike. (*e*) Folds. (*f*) Stereographic projection of first motion vectors from an earthquake. (*g*) Relation of stress directions to bore-hole breakouts.

mately along the great circle bisecting the angle between the dividing great circles in the extension first motion field. The direction of σ_3 is the perpendicular to the plane of σ_1 and σ_2. (Stereographic projection principles are presented in Appendix 5.)

Another approach to determining stress directions comes from the occurrence of rock breakage on the walls of wells and boreholes, which tends to create diametrically opposed zones of enlargement, termed "breakouts." These features can be seen in caliper logs, photographs, and televiewer logs of boreholes and have been found to be aligned from hole to hole in a region. Haimson and Herrick (1985) reported experimental results confirming that breakouts occur along the ends of a borehole diameter aligned with the least horizontal stress as depicted in Figure 4.8*g*.

Directions of horizontal stresses in the continental United States, inferred from a variety of techniques, are shown in Figure 4.7*c*, prepared by Zoback and Zoback (1988). This map also indicates the styles of deformation, that is, *extension* with the least principal stress horizontal or *contraction* with the greatest principal stress horizontal.

4.3 Techniques for Measurement of In-Situ Stresses

Stresses in situ can be measured in boreholes, on outcrops, and in the walls of underground galleries as well as back calculated from displacements measured underground. The available techniques summarized in Table 4.2 involve a variety of experimental approaches, with an even greater variety of measuring tools. Three of the best known and most used techniques are *hydraulic fracturing*, the *flat jack method*, and *overcoring*. As will be seen, they are complementary to each other, each offering different advantages and disadvantages. All stress measurement techniques perturb the rock to create a response that can then be measured and analyzed, making use of a theoretical model, to estimate part of the in situ stress tensor. In the hydraulic fracturing technique, the rock is cracked by pumping water into a borehole; the known tensile strength of the rock and the inferred concentration of stress at the well bore are processed to yield the initial stresses in the plane perpendicular to the borehole. In the flat jack test, the rock is partly unloaded by cutting a slot, and then reloaded; the in situ stress normal to the slot is related to the pressure required to null the displacement that occurs as a result of slot cutting. In the overcoring test, the rock is completely unloaded by drilling out a large core sample, while radial displacements or surface strains of the rock are monitored in a central, parallel borehole. Analysis using an unloaded thick-walled cylinder model yields stress in the plane perpendicular to the borehole. In each case stress is inferred, but

Table 4.2 *Methods for Measuring the Absolute State of Stress in Rocks*

Principle	Procedure	Reference
Complete strain relief	Overcore a radial deformation gage in a central borehole (U. S. Bureau of Mines method)	Merrill and Peterson (1961)
	Overcore a soft inclusion containing strain gages (LNEC and CSIRO methods)	Rocha et al. (1974), Worotnicki and Walton (1976)
	Overcore a borehole with strain gages on its walls (Leeman method)	Leeman (1971), Hiltscher et al. (1979)
	Drill around a rosette gage placed on a rock face	Olsen (1957)
	Overcore a rosette gage placed on the bottom of a drill hole (doorstopper method)	Leeman (1971)
	Overcore a soft photoelastic inclusion	Riley, Goodman, and Nolting 1977)
	Measure time dependent strains on faces of a rock after its removal from the ground	Emery (1962) Voight (1968)
Partial strain relief	Null displacements caused by cutting a tabular slot in a rock wall (flat jack method)	Bernède (1974) Rocha et al. (1966)
	Overcore a stiff photoelastic inclusion with down-hole polariscope (glass stress meter)	Roberts et al. (1964, 1965)
	Overcore a stiff inclusion to freeze stresses into it; measure frozen streses in the laboratory (cast inclusion method)	Riley, Goodman, and Nolting (1977)
	Overcore a stiff instrumented inclusion (stiff inclusion method)	Hast (1958) Nichols et al. (1968)
	Drill in the center of a rosette array on the surface of a rock face (undercoring method)	Duvall, in Hooker et al. (1974)
	Monitor radial displacements on deepening a borehole (borehole deepening method)	De la Cruz and Goodman (1970)
Rock flow or fracture	Measure strain to fracture a borehole with a borehole jack (Jack fracturing technique)	De la Cruz (1978)
	Measure water pressures to create and extend a vertical fracture in a borehole (Hydraulic fracturing)	Fairhurst (1965) Haimson (1978)
	Measure strains that accumulate in an elastic inclusion placed tightly in a viscoelastic rock	
	Core disking—observe whether or not it has occurred	Obert and Stephenson (1965)
Correlation between rock properties and stress; other techniques	Resistivity	
	Rock noise (Kaiser effect)	Kanagawa, Hayashi, and Nakasa (1976)
	Wave velocity	
	X-ray lattice spacing measurements in quartz	Friedman (1972)
	Dislocation densities in crystals	

displacements are actually measured. Precisions are seldom great and the results are usually considered satisfactory if they are internally consistent and yield values believed to be correct to within about 50 psi (0.3 MPa). The main problem of all stress measurement techniques is that the measurement must be conducted in a region that has been disturbed in the process of gaining access for the measurement; this paradox is handled by accounting for the effect of the disturbance in the analytical technique, as shown below.

HYDRAULIC FRACTURING

The hydraulic fracturing method makes it possible to estimate the stresses in the rock at considerable depth using boreholes. Water is pumped into a section of the borehole isolated by packers. As the water pressure increases, the initial compressive stresses on the walls of the borehole are reduced and at some points become tensile. When the stress reaches $-T_0$, a crack is formed; the down-hole water pressure at this point is p_{c1} (Figure 4.9*a*). If pumping is contin-

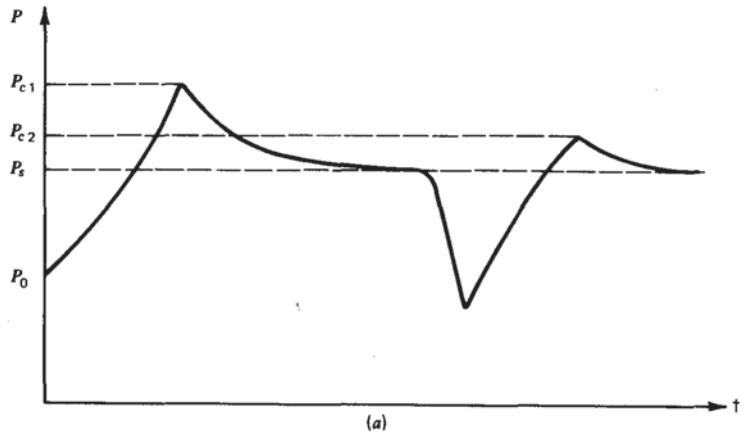

Figure 4.9 Hydraulic fracturing. (*a*) Pressure versus time data as water is pumped into the packed-off section. (*b*) Experiment in progress. (Photo by Tom Doe.)

ued, the crack will extend, and eventually the pressure down the hole will fall to a steady value p_s, sometimes called "the shut-in pressure."

To interpret the data from the hydraulic fracturing experiment in terms of initial stresses, we need to determine the orientation of the hydraulically induced fracture ("hydrofac"). The greatest amount of information coincides with the case of a vertical fracture, and this is the usual result when conducting

tests below about 800 m. The orientation of a fracture could be observed by using down-hole photography or television; however, a crack that closes upon depressuring the hole to admit the camera would be difficult to see in the photograph. It is better to use an impression packer, such as one available from Lynes Company, which forces a soft rubber lining against the wall while internal pressure is maintained, recording the fracture as an impression on the rubber surface.

The analysis of the pressure test is simplified if it is assumed that penetration of the water into the pores of the rock has little or no effect on the stresses around the hole. Making such an assumption, it is possible to use the results of the known distribution of stress around a circular hole in a homogeneous, elastic, isotropic rock (the "Kirsch solution") to compute the initial stresses at the point of fracture. The tangential stress on the wall of the hole reaches the least magnitude at A and A' (Figure 4.10) where it is

$$\sigma_\theta = 3\sigma_{h,\min} - \sigma_{h,\max} \tag{4.7}$$

When the water pressure in the borehole is p, a tensile stress is added at all points around the hole equal (algebraically) to $-p$. The conditions for a new, vertical tensile crack are that the tensile stress at point A should become equal to the tensile strength $-T_0$. Applying this to the hydraulic fracturing experiment yields as a condition for creation of a hydraulic fracture

$$3\sigma_{h,\min} - \sigma_{h,\max} - p_{c1} = -T_0 \tag{4.8}$$

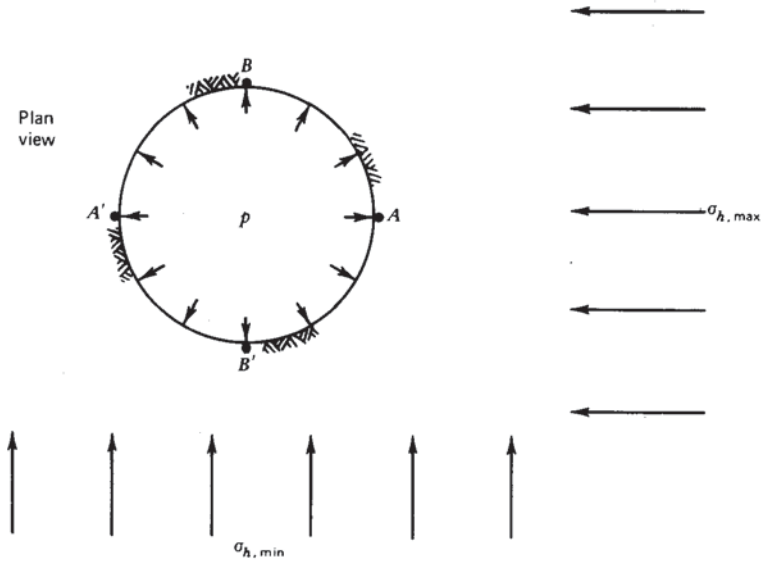

Figure 4.10 Location of critical points around the borehole used for hydraulic fracture.

Once formed, the crack will continue to propagate as long as the pressure is greater than the stress normal to the plane of the fracture. If the pressure of water in the crack were less than or greater than the normal stress on this crack, it would close or open accordingly. In rocks, cracks propagate in the plane perpendicular to σ_3. In the context of hydraulic fracturing with a vertical fracture, this means that the stress normal to the plane of the fracture is equal to the shut-in pressure p_s:

$$\sigma_{h,\min} = p_s \tag{4.9}$$

Equations 4.8 and 4.9 allow the major and minor normal stresses in the plane perpendicular to the borehole to be determined if the tensile strength of the rock is known. If the borehole pressure is dropped and once again raised above the value p_s, the hydraulic fracture will close and then reopen. Let the new peak pressure, smaller than p_{c1}, be called p_{c2}. Replacing T_0 and p_{c1} of Equation 4.8 with the values 0 and p_{c2}, respectively, and subtracting Equation 4.8 from the resulting equation yields a formula for the tensile strength of the rock around the borehole applicable to the conditions of the experiment:

$$T_0 = p_{c1} - p_{c2} \tag{4.10}$$

Assuming that the vertical stress equals γZ, and is a principal stress, the state of stress is now completely known, for the experiment yields the values and directions of the major and minor normal stress in the plane perpendicular to the borehole.

If the rock is pervious, water will enter cracks and pores creating an internal pressure gradient whereas the theory above presumed a sudden pressure drop across the borehole wall. The effect is to lower the value of p_{c1} and round the peak of Figure 4.9. Haimson (1978) shows how to modify the analysis to solve for the principal stresses in this case.

The hydraulic fracturing experiment does not yield the above results if the fracture is horizontal. Conditions for propagation of a horizontal fracture are met if the internal pressure becomes equal to the vertical stress plus the tensile strength. Assuming that the tensile strengths for propagation of horizontal and vertical fractures are the same, the vertical fracture could form only at depths below which the vertical stress obeys

$$\sigma_v \geq (3N - 1)\sigma_{h,\max} \tag{4.11}$$

where $N = \sigma_{h,\min}/\sigma_{h,\max}$. To permit an estimate of the minimum depth for vertical fracturing, it is useful to express Equation 4.11 in terms of $\overline{K}$, the ratio of mean horizontal stress to vertical stress. In these terms, a vertical fracture will form at a depth such that $\overline{K}$ is less than $(1 + N)/(6N - 2)$ where N is $\sigma_{h,\min}/\sigma_{h,\max}$ (with N restricted to values greater than $\frac{1}{3}$). The minimum depths for a vertical fracture, corresponding to the upper and lower limits of $\overline{K}(Z)$ given in Equation 4.6, are presented for various values of N in Table 4.3. When the

Table 4.3 Minimum Depths for a Vertical Hydraulic Fracture

$\sigma_{h,\min}/\sigma_{h,\max}$ (N)	Transition Value[a] of $\overline{K} = \overline{\sigma}_h/\sigma_v$ ($\overline{K}_T$)	Minimum Depth (meters) for a Vertical Hydrofrac Assuming $Z = \left(\frac{100}{\overline{K} - 0.3}\right)$	Minimum Depth (meters) for a Vertical Hydrofrac Assuming $Z = \left(\frac{1500}{\overline{K} - 0.5}\right)$
≤0.33	∞	0	0
0.40	3.5	31	500
0.50	1.5	83	1500
0.60	1.0	143	3000
0.667	0.833	188	4505
0.70	0.773	211	5495
0.80	0.643	292	10,490
0.90	0.559	386	25,424
1.00	0.500	500	∞

[a] $\overline{K} = \frac{1 + N}{6N - 2}, N > \frac{1}{3}$.

value of N is small, or when the mean horizontal stress tends toward the lower values in the range of experience, vertical fractures can occur at shallow depths. This has in fact been experienced by the oil industry, which has produced more than a million hydrofracs for artificial stimulation of oil and gas wells.

THE FLAT JACK METHOD

Hydraulic fracturing can be performed only in a borehole. If one has access to a rock face, for example, the wall of an underground gallery, stress can be measured using a simple and dependable technique introduced by Tincelin in France in 1952. The method involves the use of flat hydraulic jacks, consisting of two plates of steel welded around their edges and a nipple for introducing oil into the intervening space. Through careful welding and the use of preshaping bends, or internal fillets, it is possible to achieve a pressure of 5000 psi or higher in such a jack without rupture. The first step is to install one or more sets of measuring points on the face of the rock. The separation of the points is typically 6 in., but must conform to the gage length of available extensometers. Then a deep slot is installed perpendicular to the rock face between the reference points (Figure 4.11*b*); this may be accomplished by drilling overlapping jackhammer holes, by using a template to guide the drill, or by diamond sawing (Rocha et al., 1966). As a result of cutting the slot, the pin separation will decrease from d_0 to a smaller value if the rock was under an initial compression normal to the plane of the slot (Figure 4.11*c*). The initial normal stresses could

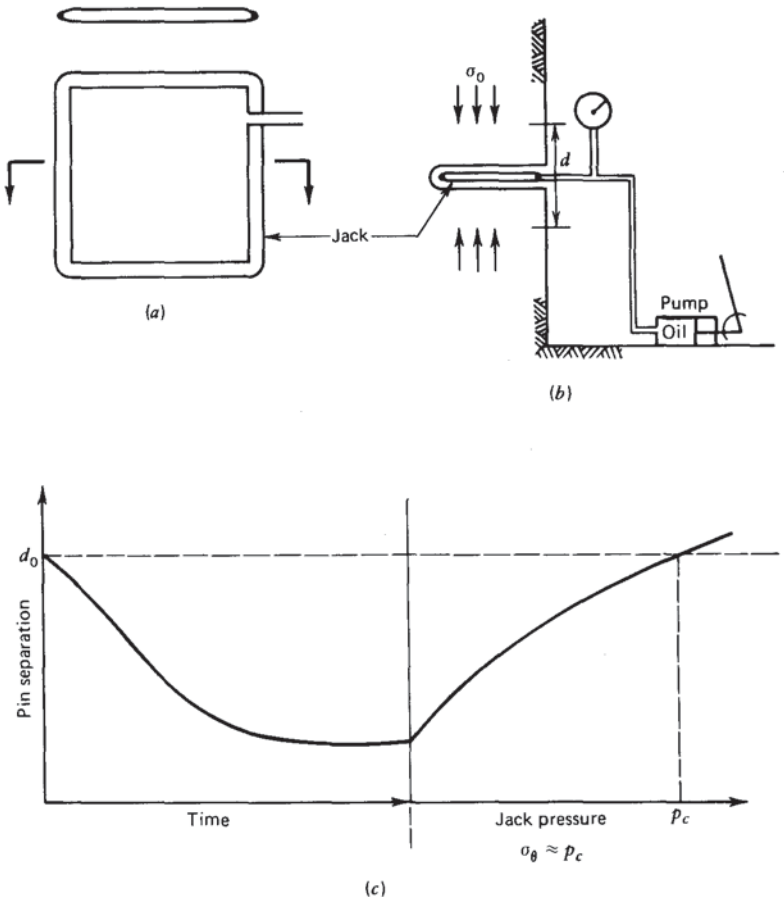

Figure 4.11 The flat jack test.

be calculated from the measured pin displacement if the elastic constants of the rock were known. However, a self-compensating method of stress determination is preferred making it unnecessary to determine the rock properties explicitly. The flat jack is inserted into the slot, cemented in place, and pressured. When the pins have been returned to d_0, their initial separation, the pressure in the jack (p_c) approximates the initial stress normal to the jack. In theory, the initial stress parallel to the slot and the geometric differences between the inside of the jack and the inside of the slot require a correction to this result (Alexander, 1960). However, the correction is often within the band of uncertainty anyway, and if a diamond sawed slot is used, it is negligibly small; thus p_c (the "cancellation pressure of the jack") is an acceptable estimate for the average stress normal to the jack.

In the flat jack test we have a large, rugged, and inexpensive method for determining one stress component of the stress tensor. The equipment can be fabricated on site and is virtually indestructible, an important consideration in any instrumentation or measurement program underground. A serious limitation of the method is that the measured stress lies in the region of disturbance of the gallery introduced for the purpose of taking the measurement. If the gallery is carefully executed, this disturbance might be calculated by conducting an independent stress concentration investigation, using numerical methods (e.g., the finite element method). In general, if the stresses normal to the plane of the jack are determined at three points around the section of the gallery, yielding values $\sigma_{\theta A}$, $\sigma_{\theta B}$, $\sigma_{\theta C}$ for the tangential stresses (stresses parallel to the surface of the opening) near the surface at these points, the initial stresses in the plane perpendicular to the gallery can be calculated by inverting the relationship:

$$\begin{Bmatrix} \sigma_{\theta,A} \\ \sigma_{\theta,B} \\ \sigma_{\theta,C} \end{Bmatrix} = \begin{pmatrix} a_{11} & a_{12} & a_{13} \\ a_{21} & a_{22} & a_{23} \\ a_{31} & a_{32} & a_{33} \end{pmatrix} \begin{Bmatrix} \sigma_x \\ \sigma_y \\ \tau_{xy} \end{Bmatrix} \tag{4.12}$$

where the coefficients a_{ij} are determined by the numerical study. For example, suppose flat jacks were placed at R and W, in the roof and side wall, respectively, of a perfectly circular underground opening; if the initial stresses were known to be horizontal and vertical, and if the tunnel radius were large compared to the width of the jacks, then Equation 4.12 would simplify to

$$\begin{Bmatrix} \sigma_{\theta,W} \\ \sigma_{\theta,R} \end{Bmatrix} = \begin{pmatrix} -1 & 3 \\ 3 & -1 \end{pmatrix} \begin{Bmatrix} \sigma_{\text{horiz}} \\ \sigma_{\text{vert}} \end{Bmatrix} \tag{4.13}$$

whereupon

$$\sigma_{\text{horiz}} = \tfrac{1}{8}\sigma_{\theta,W} + \tfrac{3}{8}\sigma_{\theta,R}$$

and

$$\sigma_{\text{vert}} = \tfrac{3}{8}\sigma_{\theta,W} + \tfrac{1}{8}\sigma_{\theta,R} \tag{4.14}$$

The stresses around an underground gallery vary inversely with the radius squared (see Equations 7.1). Therefore, if stresses are measured in a borehole at least one gallery diameter in depth, the results should correspond to the initial state of stress before driving the measurement gallery. This can be accomplished using the *overcoring test*.

OVERCORING

First one drills a small-diameter borehole and sets into it an instrument to respond to changes in diameter. One such instrument is the U. S. Bureau of Mines six-arm deformation gage (Figures 4.12*a* and 4.13*a*), a relatively rugged

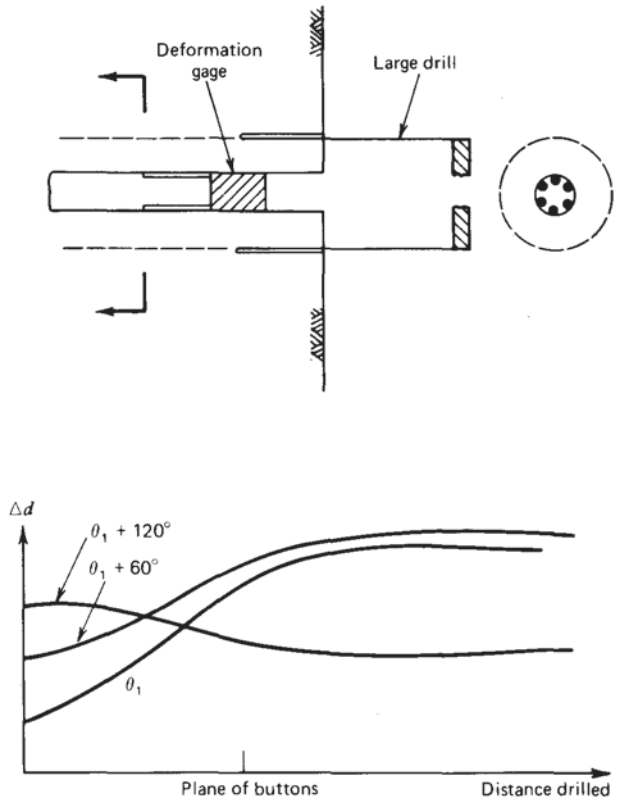

Figure 4.12 The overcoring method, using the Bureau of Mines gage.

tool that uses the bending of a cantilever equipped with strain gages to give output voltage proportional to displacement. There are three opposed pairs of carbon-carbide-tipped buttons, each pressing against a cantilever arm fixed to a base plate, tightened against the wall of the borehole by a spring. By choosing a button of appropriate size in each of the six positions, each of the cantilevers can be pre-bent to yield an initial output in the center of the linear region and the borehole diameter changes can be monitored along three diameters simultaneously, whether the borehole becomes smaller or larger. After the gage is inserted, the output wires are threaded through a hollow drill and out through the water swivel and a larger hole is cored concentrically over the first (Figure 4.13*b*). This produces a thick-walled cylinder of rock, detached from the rock mass and therefore free of stress. If the rock had been under an initial compression, the deformation gage will record an enlargement along two or all of the monitored directions in response to the "overcoring" (Figure 4.12*b*)—all radii

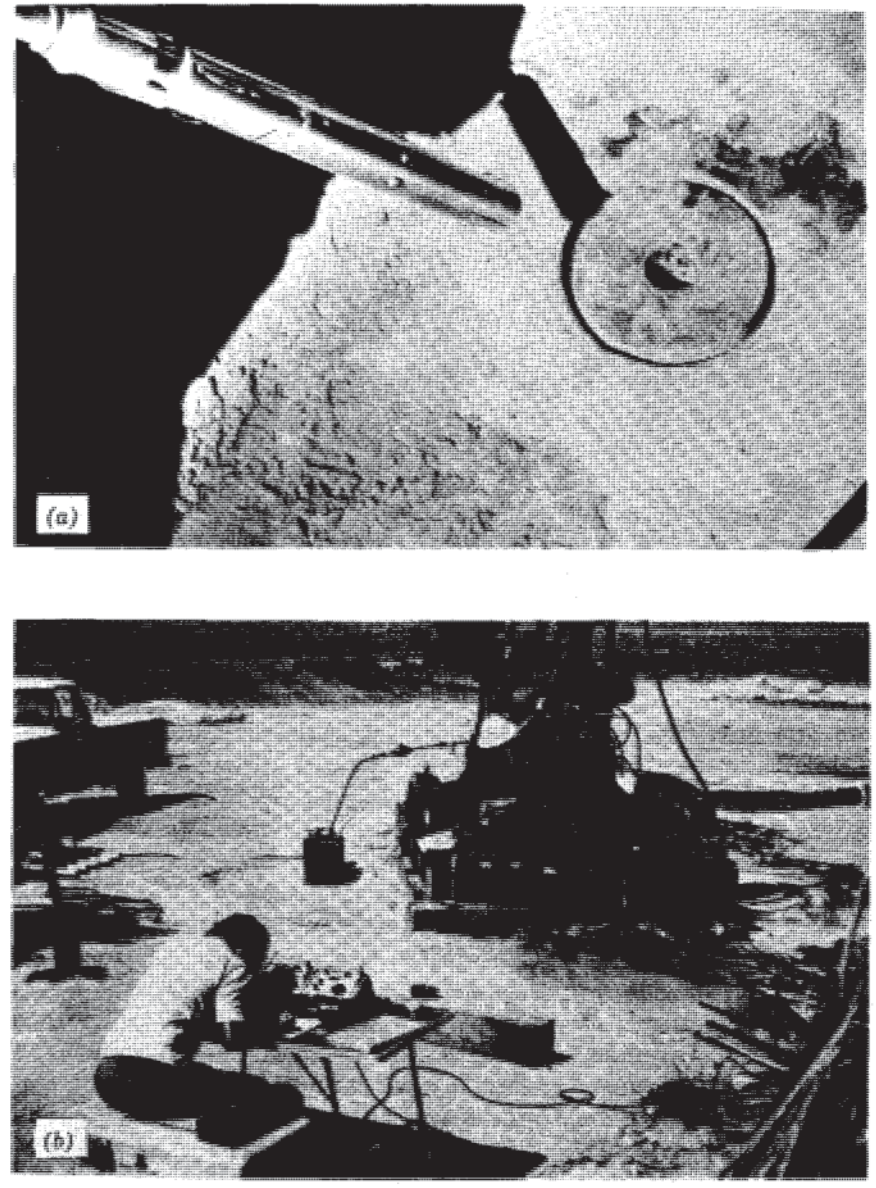

Figure 4.13 In-situ stress measurements by overcoring from a rock outcrop. (*a*) Six component borehole deformation gage and the overcored measuring hole: (*b*) experiment in progress. (Photos by Rick Nolting; Courtesy of TerraTek.)

expanding if the ratio of minor to major normal stress in the plane perpendicular to the borehole is greater than one-third. As a result of the experiment, the change in borehole diameter will be known along three diameters, 60° apart. Select an x axis conveniently in the plane perpendicular to the hole and let θ be the angle counterclockwise from $0x$ to a pair of buttons that yields results $\Delta d(\theta)$. Let the plane perpendicular to the borehole be the xz plane, with the borehole parallel to y. Then, the deformations measured are related to the initial stresses in the xyz coordinate system according to

$$\Delta d(\theta) = \sigma_x f_1 + \sigma_y f_2 + \sigma_z f_3 + \tau_{xz} f_4 \tag{4.15}$$

where $f_1 = d(1 + 2\cos 2\theta)\dfrac{1 - \nu^2}{E} + \dfrac{d\nu^2}{E}$

$$f_2 = -\frac{d\nu}{E}$$

$$f_3 = d(1 - 2\cos 2\theta)\frac{1 - \nu^2}{E} + \frac{d\nu^2}{E}$$

$$f_4 = d(4\sin 2\theta)\frac{1 - \nu^2}{E}$$

In the above, E is Young's modulus, ν is Poisson's ratio, and d is the diameter of the borehole in which the measurement is conducted. Equation 4.15 excludes the two shear stress components τ_{xy} and τ_{zy} parallel to the borehole because these have no influence on the diameter of the borehole. Gray and Toews (1968) showed that only three linearly independent equations are obtainable from repeated diametral measurements in different orientations, so the general state of stress cannot be computed from diameter changes recorded in one borehole. However, a solution can be found if one of the stress components is known or can be assumed. If the measurement is conducted in a borehole perpendicular to a rock face and at shallow depth, σ_y might be taken as zero. If the value of σ_y were known, or assumed, on the other hand, the term $f_2\sigma_y$ could be taken to the left side of the equal sign in each of three equations representing measurements along different directions and the remaining three stress components could be determined. In this way, the state of stress in the plane perpendicular to the borehole could be computed as a function of σ_y alone. An alternative approach, discussed later, is to combine measurements from three or more nonperpendicular boreholes, adopting a single, universal coordinate system into which the unknown stresses from each borehole are transformed. The resulting set of equations will be redundant, and, furthermore, since it is impossible to occupy the same volume of rock in more than one measurement, the results will be scattered.

In the usual situation where measurements are conducted in one borehole parallel to y, and a value of σ_y is assumed for purposes of computation, diameter change measurements are conducted in directions θ_1, $\theta_1 + 60$, and $\theta_1 + 120$, yielding three equations in three unknowns:

$$\begin{Bmatrix} \Delta d(\theta_1) - f_2\sigma_y \\ \Delta d(\theta_1 + 60) - f_2\sigma_y \\ \Delta d(\theta_1 + 120) - f_2\sigma_y \end{Bmatrix} = \begin{pmatrix} f_{11} & f_{13} & f_{14} \\ f_{21} & f_{23} & f_{24} \\ f_{31} & f_{33} & f_{34} \end{pmatrix} \begin{Bmatrix} \sigma_x \\ \sigma_z \\ \tau_{xz} \end{Bmatrix} \tag{4.16}$$

Inversion of Equations 4.16, after assuming a value for σ_y, yields the stress components in the plane perpendicular to the borehole.

The overcoring test thus can be used to measure the stresses at some distance from a rock face. There is a practical limit to how far one borehole can be drilled concentrically over another. With a template to collar the drillhole and homogeneous, nonfractured rock, it might be possible to proceed for as much as 30 m from a face; but normally the test has to be discontinued beyond about 5 m.

The Swedish State Power Board has perfected the mechanical aspects of overcoring and has succeeded in conducting Leeman-type triaxial measurements at depths of more than 500 m. These tests are performed by cementing strain gage rosettes to the walls of a 36-mm hole drilled exactly in the center of the bottom of a 76-mm-diameter borehole. Extending the larger borehole overcores the former and strains the rosettes (Hiltscher, Martna, and Strindell, 1979; Martna, Hiltscher, and Ingevald 1983).

The principal disadvantage of the U. S. Bureau of Mines overcoring test is the linear dependence of the stresses upon the elastic constants. The Bureau of Mines determines E and ν directly on the overcore by compressing it in a special large-diameter triaxial compression chamber, while the borehole deformation gage responds inside. Another approach, applicable in horizontal holes, is to assume a value for ν and use the value of E that makes the vertical component of stress, at some distance behind the wall, agree with the value of the unit weight of rock times depth below ground. Another approach altogether is to replace the deformation gage with a stiffer gage (e.g., glass or steel) forming a "stiff elastic inclusion." In such a case, the stresses inside the inclusion on overcoring are almost independent of the elastic modulus of the rock. However, the precision of measurement is reduced making the experiment more difficult. Another difficulty with the overcoring method is the requirement to use large drill cores (e.g., 6-in.-diameter). There is no theoretical demand that the outer diameter be any specific value, and, in fact, the stresses deduced from the experiment will be unaffected by choice of outer diameter. In practice, however, difficulty is experienced with rock breakage if the outer diameter is less than at least twice the inner diameter.

In the *doorstopper method* (Figure 4.14) strain gages are fixed to the center of the stub of rock at the bottom of the hole which is then isolated from the surrounding rock by continuing the original hole (Leeman, 1971). This permits

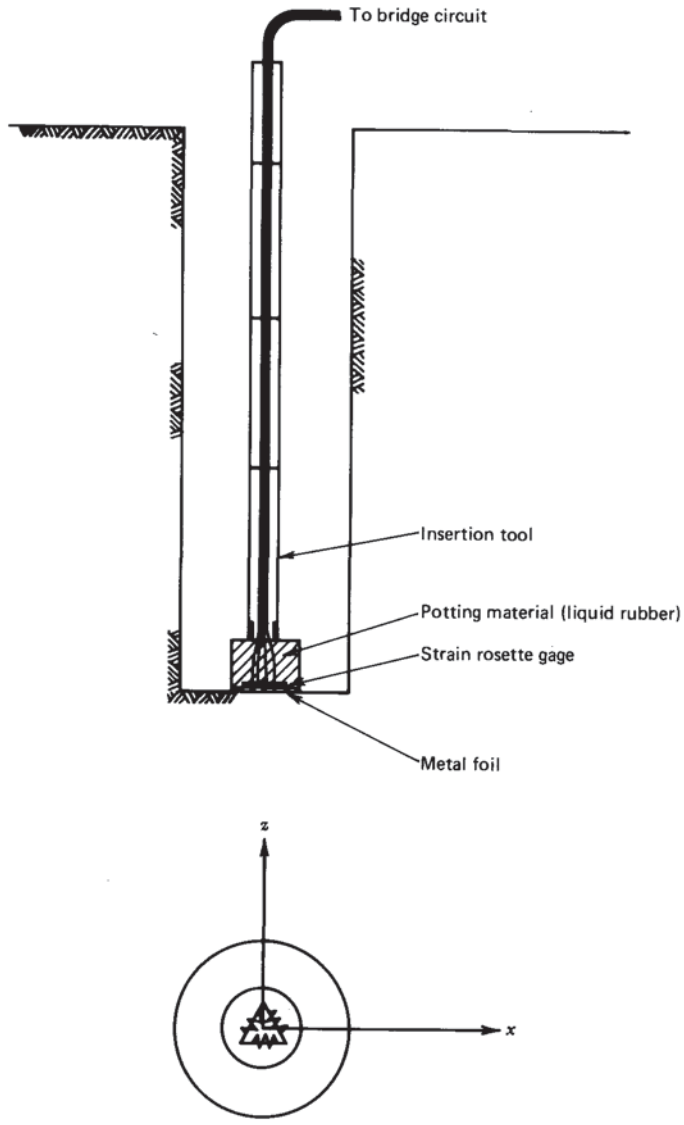

Figure 4.14 In situ stress measurement by the "doorstopper" technique.

the interpretation of stress at greater depth but the interpretation of the data is more precarious. The test is performed as follows. First, drill a borehole to the site of measurement. Then install a flat, noncoring drill bit to grind the bottom to a smooth flat surface. Clean the bottom surface and then cement onto it a piece of metal foil bearing a strain gage rosette on its upper surface. When the cement has hardened, thread the bridge wires through the drill and deepen the hole. This releases the stresses in the bottom, yielding strains ε_x, ε_z, γ_{xz} (with the y axis parallel to the borehole and the x, z axes along two perpendicular lines in the bottom, selected at will). Appendix 2 shows how to convert strain rosette readings to strain components ε_x, ε_z, γ_{xz}.

The changes in stress at the bottom of the hole ($\Delta\sigma_{x,B}$, $\Delta\sigma_{y,B}$, $\Delta\tau_{xy,B}$) can be calculated from the strain components by the stress-strain relationship for linear, elastic isotropic bodies:

$$\begin{Bmatrix} \Delta\sigma_{x,B} \\ \Delta\sigma_{z,B} \\ \Delta\tau_{xz,B} \end{Bmatrix} = \frac{E}{1-\nu^2} \begin{bmatrix} 1 & \nu & 0 \\ \nu & 1 & 0 \\ 0 & 0 & \dfrac{1-\nu}{2} \end{bmatrix} \begin{Bmatrix} \varepsilon_x \\ \varepsilon_z \\ \gamma_{xz} \end{Bmatrix} \tag{4.17}$$

The initial stresses in x, y, z coordinates are related to the stress changes on the bottom of the hole by

$$\begin{Bmatrix} \Delta\sigma_{x,B} \\ \Delta\sigma_{z,B} \\ \Delta\tau_{xz,B} \end{Bmatrix} = -\begin{pmatrix} a & c & b & 0 \\ b & c & a & 0 \\ 0 & 0 & 0 & d \end{pmatrix} \begin{Bmatrix} \sigma_x \\ \sigma_y \\ \sigma_z \\ \tau_{xz} \end{Bmatrix} \tag{4.18}$$

Constants a, b, c, and d have been evaluated by several independent workers. De la Cruz and Raleigh (1972) give the following values, based upon a finite element analysis:

$$\begin{aligned} a &= 1.30 \\ b &= (0.085 + 0.15\nu - \nu^2) \\ c &= (0.473 + 0.91\nu) \\ d &= (1.423 - 0.027\nu) \end{aligned} \tag{4.19}$$

As in the overcoring test, σ_y must be assumed or evaluated independently. Then

$$\begin{Bmatrix} \sigma_x \\ \sigma_z \\ \tau_{xz} \end{Bmatrix} = -\begin{pmatrix} a & b & 0 \\ b & a & 0 \\ 0 & 0 & d \end{pmatrix}^{-1} \begin{Bmatrix} \Delta\sigma_{x,B} + c\sigma_y \\ \Delta\sigma_{z,B} + c\sigma_y \\ \Delta\tau_{xz,B} \end{Bmatrix} \tag{4.20}$$

The "doorstopper" method can be pursued at the bottom of a shaft as well as in a drill hole.

Measurements Made Directly on the Rock Surface If a machine-bored shaft or tunnel is available for rock mechanics work, stress measurements may be made directly on the wall if the rock is not highly fractured. There are at least two methods for doing this: overdrilling a strain gage *rosette* applied directly to the rock surface, and drilling a central hole amid a set of measuring points (*undercoring*).

Strain gage rosettes applied to the rock surface have been used in boreholes by Leeman (1971) with an ingenious device to transport, glue, and hold the rosettes at several points simultaneously. Upon overcoring the hole, these rosettes then report strain changes that can be transformed to yield the complete state of stress $(\sigma)_{xyz}$. In the present context, we can overcore strain gage rosettes cemented to points directly on the rock surface. Appendix 2 presents formulas for calculating the state of strain (ε_x, ε_z, γ_{xz}) from the readings of the component gages of the rosette when the rock to which they are attached is overcored. These strains can then be converted to stresses using (4.17).

Undercoring is a name applied by Duvall (in Hooker et al., 1974) to a procedure for measuring stresses on an exposed surface by monitoring radial displacements of points around a central borehole (Figure 4.15). Expressions for the radial and tangential displacements of a point located at polar coordinates r, θ from the central hole of a radius a are given in Equations 7.2 for plane strain; these expressions are changed to plane stress by substituting $v/(1 + \nu)$ in place of ν as discussed in the derivation of Equations 7.1 and 7.2 (Appendix 4).

Equations 7.2 are developed for the condition where the major and minor principal stress directions in the measuring plane are known. For the stress measurement problem, these directions will not be known apriori so an arbi-

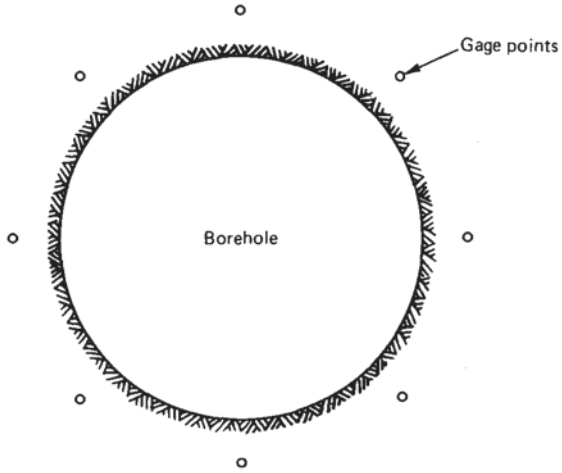

Figure 4.15 Undercoring.

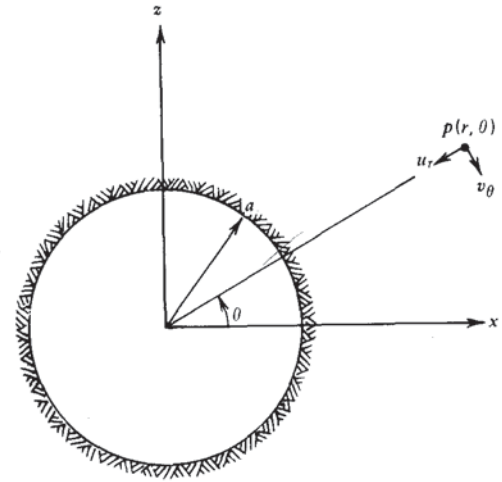

Figure 4.16 Coordinate system for the displacement equations.

trary choice of axes (x, z) is made (Figure 4.16). The stresses $\{\sigma\}_{xz}$ can then be determined from radial displacement measurements (u_r) at three positions (r, θ) using the following equation for each point in turn[3]:

$$u_r = \sigma_x f_1 + \sigma_z f_2 + \tau_{xz} f_3 \tag{4.21}$$

where $$f_1 = \frac{1}{2E}\frac{a^2}{r}[(1 + \nu) + H \cos 2\theta]$$

$$f_2 = \frac{1}{2E}\frac{a^2}{r}[(1 + \nu) - H \cos 2\theta]$$

$$f_3 = \frac{1}{E}\frac{a^2}{r}(H \sin 2\theta)$$

$$H = 4 - (1 + \nu)\frac{a^2}{r^2}$$

With radial displacement, $u_{r,1}$ measured at r_1, θ_1, $u_{r,2}$ at r_2, θ_2, and $u_{r,3}$ at r_3, θ_3, Equation 4.21 yields

$$\begin{Bmatrix} u_{r,1} \\ u_{r,2} \\ u_{r,3} \end{Bmatrix} = \begin{bmatrix} f_{11} & f_{12} & f_{13} \\ f_{21} & f_{22} & f_{23} \\ f_{31} & f_{32} & f_{33} \end{bmatrix} \begin{Bmatrix} \sigma_x \\ \sigma_z \\ \tau_{xz} \end{Bmatrix} \tag{4.22}$$

[3] We assume that the tangential displacement v_θ does not influence the measured radial displacement.

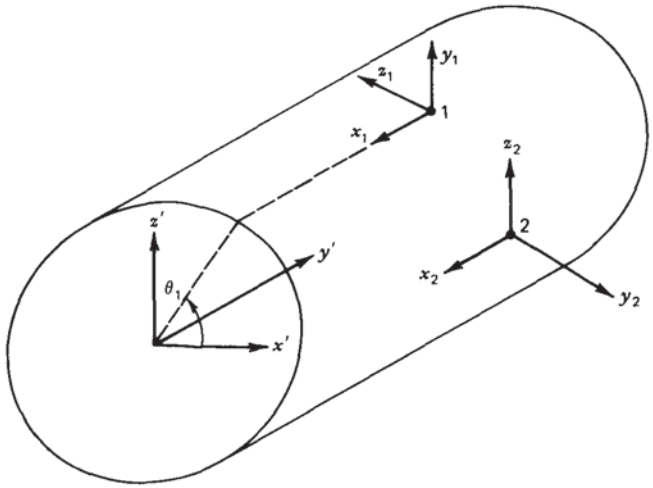

Figure 4.17 Coordinate systems for stress measurements on the walls of a tunnel.

which can be inverted to determine the stresses. This method cannot yield good percision unless the measuring points are close to the surface of the central hole, or the rock is deformable; otherwise, the values of u_r will be quite small. Duvall placed the measuring pins on a 10-in.-diameter circle and created a 6-in. central hole by reaming out an *EX* pilot hole. Vojtec Mencl used undercoring to measure stresses in the toe of a landslide in soft rock,[4] where measurable displacements were experienced despite relatively small stresses (0.6 MPa) because the value of E was quite low. A variant of undercoring using a central cylindrical expansion cell (dilatometer) to null the initial radial displacements of points around the central hole was used by Dean, Beatty, and Hogan at Broken Hill Mine, Australia.[5]

Virgin stresses (the initial stresses at the test site before it was excavated) can be calculated from the stress components measured on the rock walls if the stress concentrations at the measuring points are known. The problem at hand resembles that discussed previously in connection with the flat jack test. Since the shape of the bored gallery is circular with smooth walls, the required stress concentrations can be obtained from the classical Kirsch solution (whose derivation can be followed in Jaeger and Cook (1976)). For our purposes, the adopted coordinate system is shown in Figure 4.17; unprimed coordinates

[4] O. Zaruba and V. Mencl (1969) *Landslides and Their Control*, Elsevier, New York.

[5] Rock stress measurements using cylindrical jacks and flat jacks at North Broken Hill Ltd. from *Broken Hill Mine Monography No. 3* (1968), Australian Inst. Min. Metal. Melbourne, Australia (399 Little Collins St.).

$x_1y_1z_1$, $x_2y_2z_2$, etc., refer to local coordinate directions at each measuring site 1, 2, etc., with y_1y_2 . . . always in the direction of the normal to the surface (radius of the tunnel or shaft) and x_1x_2, etc., parallel to the axis of the measuring tunnel or shaft. The x', y', z' are global coordinates with y' parallel to the axis of the shaft or tunnel, and x' and z' any convenient orthogonal axes in its cross section.

The surface stress concentrations can then be obtained from the general Kirsch formulas given by Leeman (1971) (see Appendix 4), substituting $r = a$ to identify points on the wall at the site of the measurement: with the above coordinates, at each site

$$\begin{aligned} \sigma_r &= \sigma_y = 0 \\ \sigma_\theta &= \sigma_z \\ \sigma_{\text{long}} &= \sigma_x \\ \tau_{r\theta} &= \tau_{yz} = 0 \\ \tau_{\text{long},\theta} &= \tau_{xz} \\ \tau_{\text{long},r} &= \tau_{xy} = 0 \end{aligned}$$

$$\begin{Bmatrix} \sigma_z \\ \sigma_x \\ \tau_{xz} \end{Bmatrix} = \begin{pmatrix} d & 0 & e & 0 & 0 & f \\ g & 1 & h & 0 & 0 & i \\ 0 & 0 & 0 & n & p & 0 \end{pmatrix} \begin{Bmatrix} \sigma_{x'} \\ \sigma_{y'} \\ \sigma_{z'} \\ \tau_{x'y'} \\ \tau_{y'z'} \\ \tau_{z'x'} \end{Bmatrix} \tag{4.23}$$

where $d = 1 - 2\cos 2\theta$ $\quad h = 2\nu \cos 2\theta$

$e = 1 + 2\cos 2\theta$ $\quad i = -4\nu \sin 2\theta$

$f = -4 \sin 2\theta$ $\quad n = -2 \sin \theta$

$g = -2\nu \cos 2\theta$ $\quad p = 2 \cos \theta$

Two or more sites for surface stress measurement (e.g., (1) the roof $\theta_1 = 90°$, and (2) the wall $\theta_2 = 0$ (Figure 4.17) yield six equations whose solution determines the complete state of stress. Depending on the choice of sites, the coefficient matrix might be singular, necessitating a third location (with redundant data) to obtain a complete stress solution.

Principal Stresses If the stresses are determined with reference to two arbitrarily chosen directions x and z in the plane of measurement, the values of normal stress will depend on the choice of axes. It is better to convert the results to the form of principal stresses and directions. (If the xz plane is not a principal plane, it is still possible to find, within it, directions in which the shear

stress is zero; these are then called "secondary principal stresses.") Given σ_x, σ_z, and τ_{xz}, the principal stresses are found from

$$\sigma_{\text{major}} = \tfrac{1}{2}(\sigma_x + \sigma_z) + [\tau_{xz}^2 + \tfrac{1}{4}(\sigma_x - \sigma_z)^2]^{1/2}$$

and (4.24)

$$\sigma_{\text{minor}} = \tfrac{1}{2}(\sigma_x + \sigma_z) - [\tau_{xz}^2 + \tfrac{1}{4}(\sigma_x - \sigma_z)^2]^{1/2}$$

The major principal stress, σ_1 acts in a direction θ, measured counterclockwise from $0x$, given by

$$\tan 2\theta = \frac{2\tau_{xz}}{\sigma_x - \sigma_z} \tag{4.25}$$

Since the arctan is multivalued, we must observe the following rules.[6] Let $\alpha = \tan^{-1}[2\tau_{xz}/(\sigma_x - \sigma_z)]$ with $-\pi/2 \le \alpha \le \pi/2$ then

$$\begin{aligned} 2\theta &= \alpha && \text{if } \sigma_x > \sigma_z \\ 2\theta &= \alpha + \pi && \text{if } \sigma_x < \sigma_z \text{ and } \tau_{xz} > 0 \\ 2\theta &= \alpha - \pi && \text{if } \sigma_x < \sigma_z \text{ and } \tau_{xz} < 0 \end{aligned}$$

Measurement of Stresses in Three Dimensions Civil engineering and mining work rarely require that all stress components be known. If such knowledge is desired, methods exist to yield the complete state of stress from a single experiment (e.g., Leeman, 1971; Rocha et al., 1974). Also, data from techniques enumerated above can be combined to permit computation of the complete stress matrix. A procedure for doing this was already discussed for the case of strain measurements on the surface of a drilled shaft or tunnel. Data can also be combined for overcoring, doorstopper, and other approaches. In each case, the strategy is to transform the measured stress components to a global coordinate system to combine data from nonparallel directions at different measuring sites.

For example, consider overcoring measurements in several nonparallel boreholes. In hole A, adopt coordinate axes x_A, y_A, z_A with y_A parallel to the axis of the borehole; diametral displacements are measured in directions θ_{A1}, θ_{A2}, and $\theta_{A,3}$. Application of 4.15 to each direction yields

$$\begin{Bmatrix} \Delta d(\theta_{A,1}) \\ \Delta d(\theta_{A,2}) \\ \Delta d(\theta_{A,3}) \end{Bmatrix} = \begin{pmatrix} f_{11} & f_{12} & f_{13} & f_{14} \\ f_{21} & f_{22} & f_{23} & f_{24} \\ f_{31} & f_{32} & f_{33} & f_{34} \end{pmatrix} \begin{Bmatrix} \sigma_{x,A} \\ \sigma_{y,A} \\ \sigma_{z,A} \\ \tau_{xz,A} \end{Bmatrix} \tag{4.26}$$

[6] These rules were suggested to the writer by Professor Steven Crouch, University of Minnesota.

where the coefficients f_{ij} are defined for each θ for f_j of (4.15). Now transform the stresses in $x_A y_A z_A$ coordinates to some convenient set of axes x', y', z' (referred to henceforth as the "global axes"). This can be written

$$\underset{(4\times 6)}{\begin{Bmatrix} \sigma_{x,A} \\ \sigma_{y,A} \\ \sigma_{z,A} \\ \tau_{xz,A} \end{Bmatrix}} = \underset{(4\times 6)}{(T_\sigma)} \underset{(6\times 1)}{\{\sigma\}_{x'y'z'}} \tag{4.27}$$

in which (T_σ) is a 4×6 matrix corresponding to rows 1, 2, 3, and 5 of the coefficient matrix defined in Equation 23 of Appendix 1, and $\{\sigma\}_{x'y'z'}$ is the column of the six stress components of the same equation. Let (f_A) denote the 3×4 coefficient matrix in (4.26). Equations 4.26 and 4.27 can then be combined into

$$\underset{3\times 1}{\{\Delta d\}_A} = \underset{3\times 4}{(f_A)} \underset{4\times 6}{(T_\sigma)_A} \underset{6\times 1}{\{\sigma\}_{x'y'z'}} \tag{4.28}$$

Similarly for borehole B, nonparallel with A,

$$\underset{3\times 1}{\{\Delta d\}_B} = \underset{3\times 4}{(f_B)} \underset{4\times 6}{(T_\sigma)_B} \underset{6\times 1}{\{\sigma\}_{x'y'z'}} \tag{4.29}$$

Combining the six rows of (4.28) and (4.29) gives six equations with $\sigma_{x'y'z'}$ as the right-hand vector. Gray and Toews (1968), however, showed that the coefficient matrix thus derived is singular. Thus three nonparallel boreholes will be required to yield sufficient information to solve for $\{\sigma\}_{x'y'z'}$. One can reject surplus rows to achieve a solvable set of six equations. Even better, one can use a least-squares solution scheme. Panek (1966) and Gray and Toews (1975) showed how to handle the redundancy and minimize error associated with variation in the state of stress from one measuring site to another.

A similar procedure can be followed to combine the results from "doorstopper tests" in three nonparallel holes to determine the complete state of stress.

References

Alexander, L. G. (1960) Field and lab. test in rock mechanics, *Proceedings, Third Australia–New Zealand Conference on Soil Mechanics*, pp. 161–168.

Bernède, J. (1974) New Developments in the flat jack test (in French), *Proc. 3rd Cong. ISRM* (Denver), Vol. 2A, pp. 433–438.

Booker, E. W. and Ireland, H. O. (1965) Earth pressures at rest related to stress history, *Can. Geot. J.* **2**: 1–15.

Brekke, T. L. (1970) A survey of large permanent underground openings in Norway, *Proceedings of Conference on Large Permanent Underground Openings*, pp. 15–28 (Universitets Forlaget, Oslo).